



SLIDING WEAR BEHAVIOUR OF AISI 304 AUSTENITIC STAINLESS STEEL AT ELEVATED TEMPERATURE

Balamurugan G M¹, Muthukannan Duraiselvam^{2*} and Subramaniam Arunachalam³

¹Department of Mechanical Engineering, Jayaram College of Engineering and Technology, Tiruchirappalli-621014, Tamil Nadu, India.

²Department of Production Engineering, National Institute of Technology, Tiruchirappalli-620015, Tamil Nadu, India

³School of Computing, Information Technology and Engineering, 4 - 6 University Way, Beckton, London, United Kingdom

ABSTRACT

The study analyses the tribological properties of commercially available 304 Austenitic stainless steel (SS) under dry condition. Pin on disc wear test enabled to study the wear resistance and coefficient of friction on the basis of friction force obtained in the course of continuous measurement under different load (30N and 50N) and temperature (30 °C and 100°C). To study the mass loss, the weight of the disc and the pin were measured using an electronic analytical balance. Scanning electron microscope pictures of the worn surfaces were analyzed to identify the wear mechanism. The rate of wear at 100°C was higher than 30°C. As time advances, the variation of wear was progressively increased. The worn surface at 100°C shows the delaminated multiple layer with flakes, indicating the layer by layer removal of the disc. The coefficient of friction in 100°C was marginally higher due to the sliding wear at higher temperature.

Keywords: AISI 304, Sliding Wear, Load, High Temperature, SEM.

1. Introduction

Poor tribological behaviour of austenite stainless steels has been a barrier to their wider application under wear conditions. The desirable corrosion and oxidation resistance of austenitic stainless steel (ASS) led to its wide usage in various aggressive environments, typically from biomedical equipment to components in chemical, food and nuclear industries. Among austenitic stainless steels, AISI 304 (SS) have shown the lowest wear resistance both in dry sliding and under lubricated conditions due to significant mass losses [1]. The researchers have tried to enhance the wear resistance of stainless steels without losing their attractive stainless characteristics [2]. The austenitic stainless steel have an austenitic structure in annealed condition, but partially transform to martensite during deformation. The low stacking fault energy, in AISI 304 austenitic SS, makes it amenable to these transformation mechanisms by giving rise to planar faults and dislocation pile-ups [3]. The martensite is stronger and harder than the austenitic structure, causing a composite strengthening and thus a high strain hardening effect. The strain hardening effect causes higher strengths after cold working, which contributes to the high ductility in annealed condition [4]. Studies on the tribological properties of AISI 304 austenitic SS, under either high or low loading conditions in the literature [5-8] confirm such possible transformation due to friction condition.

Unfortunately, metallic counter-bodies selected in these studies would generally accelerate either their adhesion onto or the transfer tendency of the mating stainless steel. As a result, they jeopardized the relatively accurate evaluation of the friction and wear behaviour of the stainless steels. Stainless steels often display a poor tribological behaviour, which can be improved when they are hardened by incorporating N₂, TiN and Zr and forming a hardened surface zone [9].

The sliding wear of 304 austenitic SS was studied as a function of applied load (from 6 to 20N) and tangential velocity (from 0.07 to 0.81m/s). Wear experiments were conducted in a commercial pin-on-disc equipment and were designed with response surface methodology. The change in the wear mechanism was associated with the subsurface plastic deformation and surface temperature, which were strongly affected by sliding speed. In addition, strain-induced martensitic transformation was observed on the sliding surface of the austenitic stainless steels [10]. The tribological behaviour of Al-Si composite was studied. The hardness, wear resistance, co-efficient of friction and wear rate for the composites were found to depend mainly on the distribution of the primary silicon particle along the radial direction [11]. Intermetallic compounds find extensive use in high temperature structural applications. The Fe₃Al based intermetallic alloys offer unique benefits of excellent oxidation and sulfidation resistance at a potential cost lower than many stainless steels. Plasma spraying is

*Corresponding Author - E- mail: durai@nitt.edu

considered as a non-linear problem with respect to its variables: either materials or operating conditions. A mathematical technique was proposed on neural computations to study the effects of process variables on the wear behaviour of iron-aluminide coatings made by plasma spraying [12]. The effects of normal load and sliding speed on tribological properties of the metal matrix composite (MMC) pin on sliding with En 36 steel disc was evaluated. The wear rate increases with normal load and sliding speed. The wear and friction coefficient of the aluminium alloy-silicon carbide MMC is lower than the plain aluminium alloy [13]. This paper reports a study of sliding wear behaviour of AISI 304 SS sliding against EN- 24 pin under different temperature parameters. The worn surfaces are characterised by scanning electron microscope (SEM) to analyse the wear mechanism involved in the dry sliding wear experiment.

2. Experimental Procedure

The as received AISI 304 SS specimens were cut in to discs of size 100mm diameter and 4mm thickness. As received EN24 pins were prepared as 8mm diameter and 30mm height with flat ends. The chemical composition of the AISI 304 SS is Fe, <0.08% C, 17.5-20% Cr, 8-11% Ni, <2% Mn, <1% Si, <0.045% P, <0.03% S. The chemical composition of the pin material is Fe, <0.45 % C, <0.70 % Mn, < 0.35% Si, 0.90-1.40% Cr, 1.3-1.8% Ni, 0.20-0.35% Mo. The hardness values were determined by using a load of 2 kg in micro hardness tester. The Vickers hardness of 304 steel discs and the pin was 303 HV_{0.2}, 440 HV_{0.2} respectively. Experiments were conducted as per ASTM G99 - 05 Standard [14] using DUCOM pin-on-disc equipment under dry sliding test conditions. The equipment consists of a rotating spindle in which the disc was fixed. A pivoted lever arm with balancing weight and provision for fixing the pin along with the collet holder were to be brought to the desired track diameter. Desired loads were added to lever arm one by one. The test duration can be varied.

The LVDT probe was positioned on the weights to measure displacement and the load cell to sense the tangential force. The disc was washed with acetone to protect the surface normally in dry sliding condition. Fig. 1 shows the pin on disc wear testing machine. The microstructure of AISI 304 SS using the etchant nital was taken in 400 x magnification. The parameter selected for the present study is shown in Table 1. The normal loads used were 30 and 50 N. The tangential velocities were 1m/s and 2m/s and with a wear track radius of 40 mm and 70 mm respectively. The experiments were performed at 30° C and 100° C

with a constant sliding distance of 2000 m. The temperature is raised by an induction coil, which is an integral part of the equipment. Before and after test, pins and discs were ultrasonically cleaned, dried and weighed using an electronic analytical balance. Fig. 2 shows the set of samples after the dry sliding wear. Using the data acquisition system, the depth of wear and CoF were recorded automatically with respect to time. The worn surfaces were analysed using scanning electron microscope.

Fig. 1 Pin on Disc Equipment

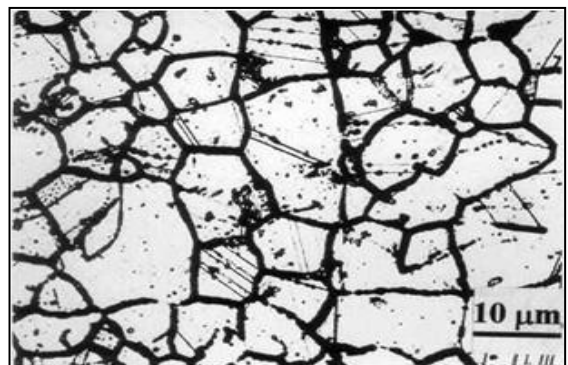


Fig. 2 Samples after Dry Sliding Wear

Table 1: Experimental Parameters

Specimen No.	Temp. (°C)	Load (N)	Velocity (m/s)
1	30	30	1
2	30	30	2
3	30	50	1
4	30	50	2
5	100	30	1
6	100	30	2
7	100	50	1
8	100	50	2

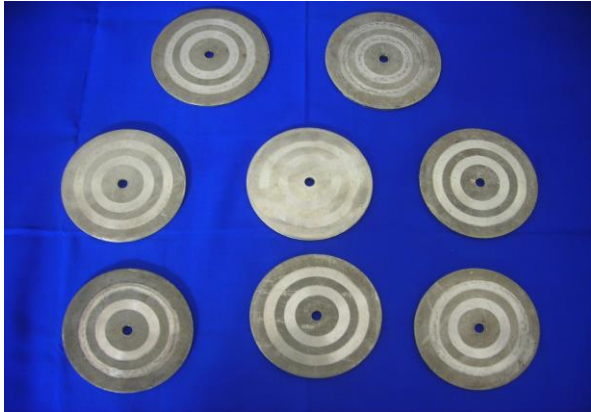


Fig. 3 Samples after Dry Sliding Wear

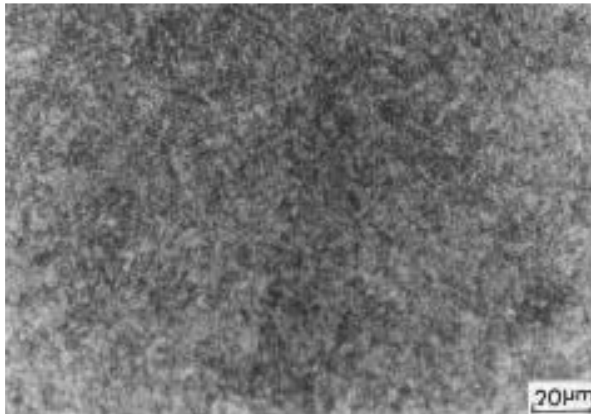


Fig. 4 Microstructure of EN 24 Pin

3. Results and Discussion

3.1 Microstructure of the disc and the pin

The Fig. 2 shows the microstructure of the AISI 304 SS with a less amount of carbides fig. 3 Shows the samples after Dry sliding wear. The Fig. 4 shows the microstructure of EN24 pin. The EN24 pin was delineated by fine tempered martensite.

3.2 Sliding wear test at room temperature and 100° C

The wear versus time graph generated by Winducom 2006 software during the wear test both at room temperature and 100°C is shown in Fig. 5. Sliding wear mechanisms were dominated by plastic deformation. The graph corresponds to parameters 30N load and 2 m/s tangential velocity. From the graph we inferred that, initially the wear at 100° C was slightly higher than that of the wear at 30°C. After that, the variation progressively increases with time. From the

frictional load, the coefficient of friction was calculated with respect to time and it was plotted in graph corresponds to parameters 30N load and 2m/s velocity which is shown in Fig. 6. It was inferred that the coefficient of friction varies between 0.5 to 0.6 in both the temperatures of 30°C and 100° C conforming the dry sliding wear action. The Coefficient of friction was progressively increases with time.

3.3 Mass loss of pin and disc

Fig. 7(a-d) shows the wear in terms of mass loss of both the pin and the disc as a function of temperature, load and velocity. It was explicit that in the velocity of 1m/s, mass loss of disc was grater than the pin mass loss. In the case of 2m/s velocity, the mass loss of pin was higher than the mass loss of the disc. The mass loss of pin increases as the load increases in higher velocity. The load and the velocity have linear relationship with the mass loss of the pin.

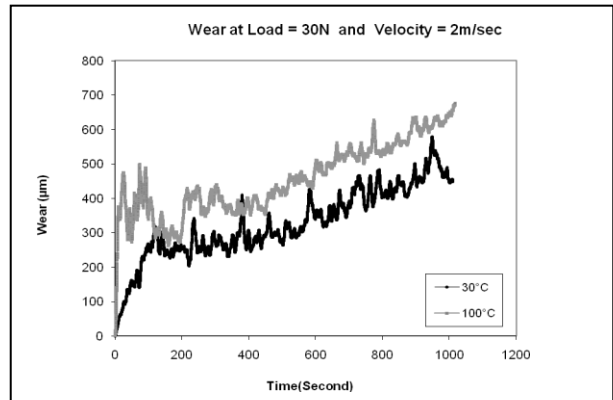


Fig. 5 Variation of Wear with Respect to Time

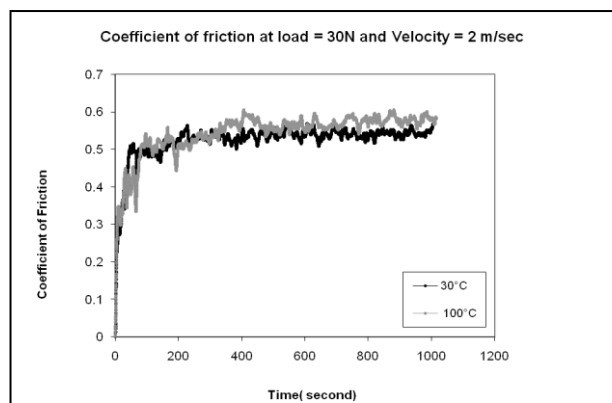
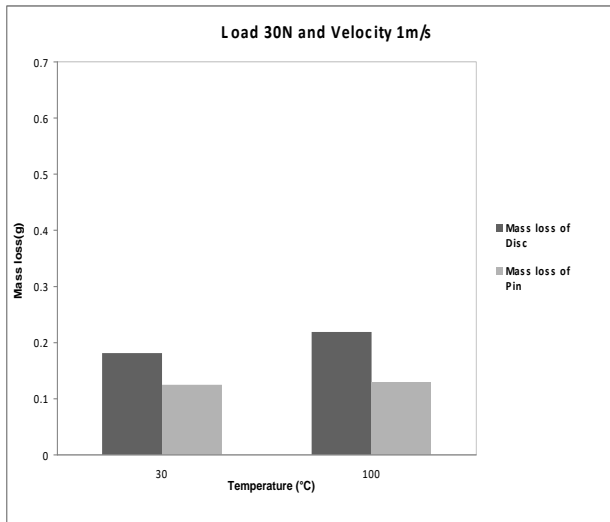
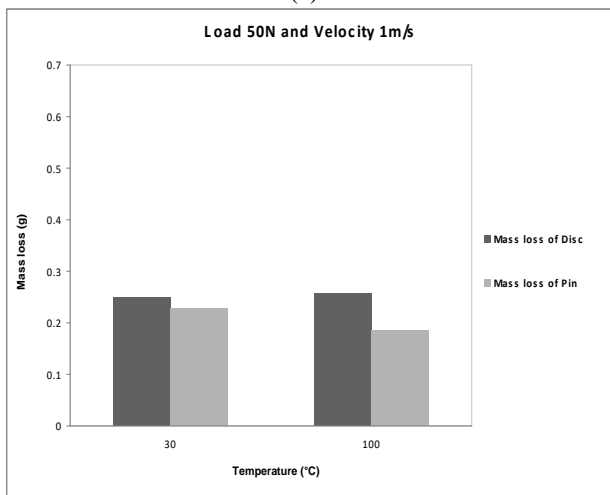


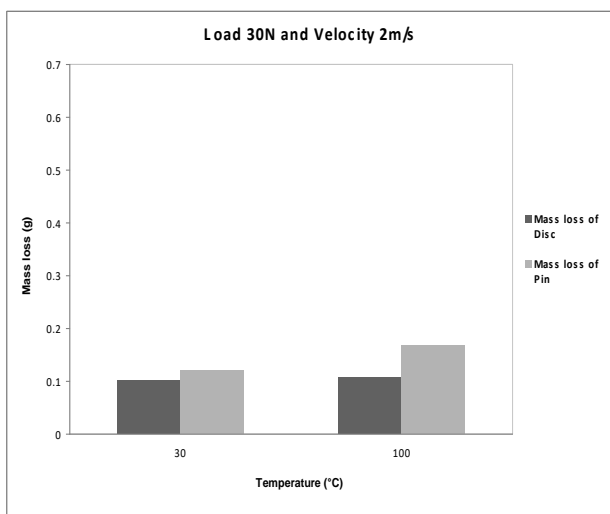
Fig. 6 Variation of Coefficient of Friction with Respect to Time



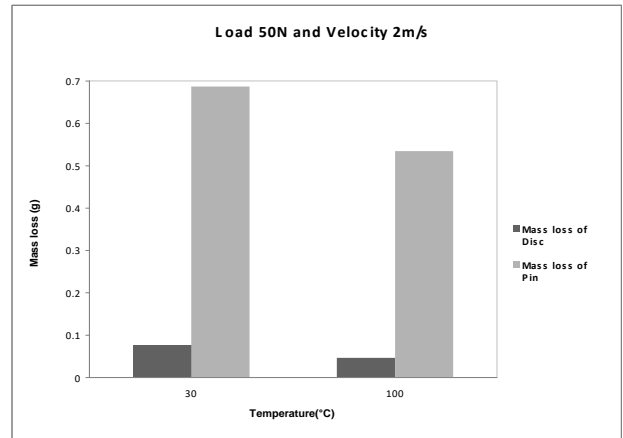
(a)



(b)



(c)



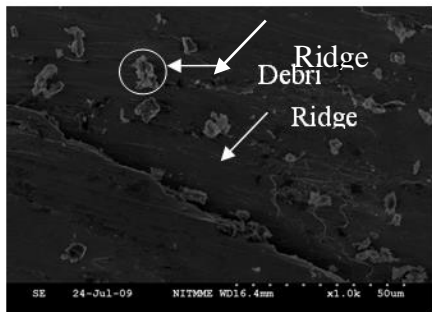
(d)

Fig. 7 (a-d) Mass Loss of Disc and Pin as a Function of Temperature, Load and Velocity

3.4 Characterization of worn surfaces

Fig. 8(a) shows the worn surface of Specimen 1. Debris and ridge was present in worn surface. Fig. 8(b) shows the worn surface of Specimen 2. A multi layered cleavage was seen in the worn surface along with small amount of debris. The worn surface was shown with evidence of a multilayered structure in the cleavage region. Fig. 9 (a) shows worn surface of Specimen 3. The sliding direction was well exposed by parallel shallow grooves. Fig. 9 (b) shows worn surface of Specimen 4.

A comparatively shallow valley was noticed and it was due to the excess material removed by the sliding wear. Materials displaced from grooves were spread over the surface allowing the chip formation and then cracks at the interface root at the edge of the groove. Fig. 10 (a) shows worn surface of Specimen 5. The surface was less grooved with the frequent flattened plateau. There was an evidence of a multilayered structure. Some of the prow surfaces were smooth with score lines while others indicated bearing areas containing numerous small contacts. Multilayered crater wear appeared clearly in the worn surface. Fig. 10 (b) shows worn surface of Specimen 6. Materials displaced laterally from grooves were spread over the surface allowing the chip formation and then cracks at the interface root at the edge of the groove. Many of these showed signs of breakdown to small debris particles. Fig. 11(a) shows worn surface of Specimen 7. The surface shows flaking wear and the same is supported by the cleavage. Fig. 11(b) shows worn surface of specimen 8. The delamination of multiple layer shown in the worn surfaces justify the layer by layer removal of the disc.

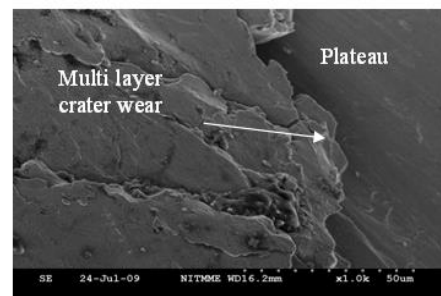


(a)

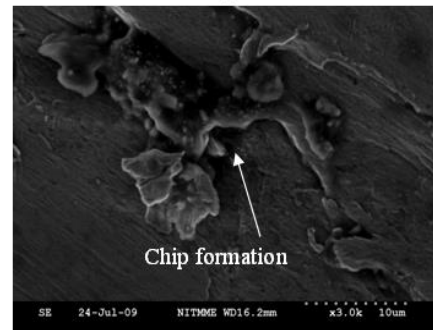


(b)

Fig. 8 SEM Micrograph of the AISI 304 Worn Surface under Load 30 N at 30°C (a) Velocity 1m/s (b) Velocity 2m/s

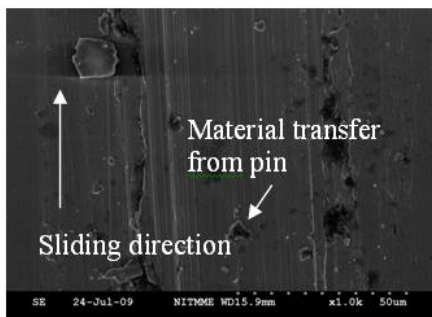


(a)

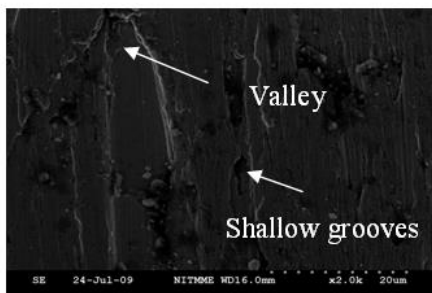


(b)

Fig. 10 SEM Micrograph of the AISI 304 Worn Surface under Load 30 N at 100°C (a) Velocity 1m/s (b) Velocity 2m/s

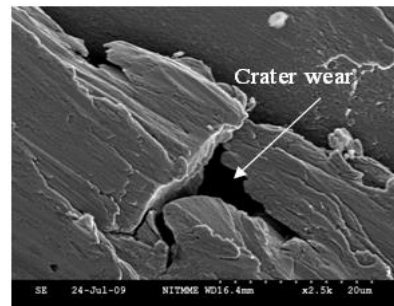


(a)

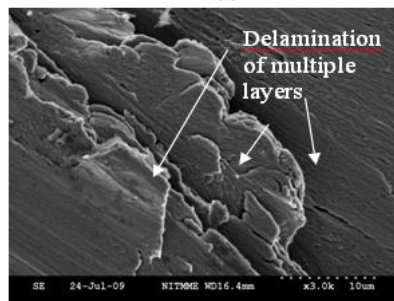


(b)

Fig. 9 SEM Micrograph of the AISI 304 Worn Surface under Load 50 N at 30°C (a) Velocity 1m/s (b) Velocity 2m/s



(a)



(b)

Fig. 11 SEM Micrograph of the AISI 304 Worn Surface under Load 50 N at 100°C (a) Velocity 1m/s (b) Velocity 2m/s

4. Conclusion

AISI 304 SS was subjected to dry sliding wear under different load, sliding velocity and temperature. Based on the experimental results, the following conclusions were drawn.

Dry sliding wear mechanisms were primarily dominated by plastic deformation. It was found that the wear in 100°C was initially higher than that of the wear in 30°C. The worn surfaces in 100°C show the delamination type of wear with flakes which becomes the reason for higher wear initially. As time progresses the variation of wear was very minimal. It was found that the coefficient of friction varies between 0.5 to 0.6. The coefficient of friction in 100°C was marginally higher due to the sliding wear at higher temperature. It was found that in all cases, the mass loss due to wear of the disc was always greater than the pin. At constant load, the mass loss of the disc decreases as the velocity increases. The slipping phenomenon may influence the reduction in wear rate at higher velocities. The higher mass loss in 100°C, under 50N load in 1m/s velocity was attributed by break up of finer particles and lateral spreading of the material which was explicit from the SEM.

References

1. Brin C, Rivière J P, Eymery J P and Villain J P (2001), "Structural Characterization of Wear Debris Produced during Friction between Two Austenitic Stainless Steel Antagonists", *Tribology Letters*, Vol. 11(2), 127–132.
2. Bell T (2002), "Surface Engineering of Austenitic Stainless Steel", *Surface Engineering*, Vol. 18(6), 415–422.
3. Amar K De, David C Murdock, Martin C Mataya, John G Speer and David K Matlock (2004), "Quantitative Measurement of Deformation-induced Martensite in 304 Stainless Steel by X-ray Diffraction", *Scripta Materialia*, Vol.50 (12), 1445–1449.
4. Zackay V F, Parker E R, Fahr D and Busch R A (1967), "The Enhancement of Ductility in High-strength Steels", *ASM Transactions Quarterly*, Vol. 60, 252–259.
5. Yang Z Y, Naylor M G S and Rigney D A (1985), "Sliding Wear of 304 and 310 Stainless Steels", *Wear* Vol. 105, 73–86.
6. Hsu K L and Ahn T M (1980), "Friction, Wear and Microstructure of Unlubricated Austenitic Stainless Steels", *Wear*, Vol. 60, 13–37.
7. Rivière J P, Brin C and Villain J P (2003), "Structure and Topography Modifications of Austenitic Steel Surfaces after Friction in Sliding Contact", *Applied Physics A: Materials Science*, Vol. 76(2), 277–283.
8. Hubner W (2001), "Phase Transformation in Austenitic Stainless Steels during Low Temperature Tribological Stressing", *Tribology International*, Vol. 34, 225–231
9. Halit Dogan, Fehim Findik, and Omer Morgul. (2002), "Friction and Wear Behaviour of Implanted 316L SS and Comparison with a Substrate", *Materials and Design*, Vol. 23(7), 605–610.
10. Farias M C M, Souza R M, Sinatora A and Tanaka D K (2007), "The Influence of Applied Load, Sliding Velocity and Martensitic Transformation on the Unlubricated Sliding Wear of Austenitic Stainless Steels", *Wear*, Vol. 263(1-6), 773–781.
11. Chikkanna N, Sankaran Kutty P and Mukunda P G (2006), "Tribological Behavior of Centrifugally Cast Al-Si Composite", *Journal of Manufacturing Engineering*, Vol.1(1), 40-44.
12. Rojaleena Das, Anupama Sahu, Chaithanya M, Mishra S C, Alok Satapathy, Ananthapadmanabhan P V and Sreekumar K P (2008), "ANN Analysis of Wear Behaviour of Plasma Sprayed Iron Aluminate Coating", *Journal of Manufacturing Engineering*, Vol. 3(2), 78-81.
13. Kathiresan M and Sornakumar T (2009), "Tribological Properties of Silicon Carbide Reinforced Aluminium Composites", *Journal of Manufacturing Engineering*, Vol. 4(2), 93-97.
14. ASTM G99-95, 1995. ASTM G99-95a (Reapproved 2000): Standard Test Method for Wear Testing with a Pin on Disc Apparatus.

